[CANCER RESEARCH 63, 5636–5645, September 1, 2003]

NADPH Oxidase Activity Is Essential for Keap1/Nrf2-mediated Induction of *GCLC* in Response to 2-Indol-3-yl-methylenequinuclidin-3-ols[1]

Konjeti R. Sekhar, Peter A. Crooks, Vijayakumar N. Sonar, David B. Friedman, Jeff Y. Chan, Michael J. Meredith, Joseph H. Starnes, Kathy R. Kelton, Samantha R. Summar, Soumya Sasi, and Michael L. Freeman[2]

Departments of Radiation Oncology [K. R. S., J. H. S., K. R. K., S. R. S., S. S., M. L. F.] and Biochemistry [D. B. F.], Vanderbilt University School of Medicine/Vanderbilt-Ingram Cancer Center, Nashville, Tennessee 37223; Department of Pharmaceutical Sciences, University of Kentucky, Lexington, Kentucky 40536 [P. A. C., V. N. S.]; Department of Pathology, University of California Irvine, Irvine, California 92697 [J. Y. C.]; and Department of Oral Molecular Biology, Oregon Health Sciences University, Portland, Oregon 97201 [M. J. M.]

ABSTRACT

Glutamate cysteine ligase, the rate-limiting enzyme for the synthesis of glutathione, represents an important component of chemoprevention paradigms. *GCLC* and *GCLM*, the genes encoding glutamate cysteine ligase subunits, are induced by indoles, such as indomethacin. Novel functionalized indole analogues and other structurally related compounds were synthesized and used for a comparative structure analysis of *GCLC* induction. Use of mouse embryo fibroblasts null for Nrf2 (nuclear factor-erythroid 2p45-related transcription factor) and HepG2 cells overexpressing Keap1 demonstrated that indole analogue-mediated *GCLC* expression was regulated by Nrf2-Keap1 interactions. Indole analogues capable of inducing *GCLC* were found to increase NADPH oxidase activity. Indole analogues unable to induce *GCLC* did not increase oxidase activity. HepG2 cells transfected with FLAG/Keap1 were exposed to indomethacin, and the redox state of Keap1 cysteine residues was assessed. The data indicated that Keap1 exhibited several oxidation states that were sensitive to indomethacin treatment. These indomethacin-mediated changes in thiol oxidation states were suppressed by diphenyleneiodonium, a NADPH oxidase inhibitor. Diphenyleneiodonium also suppressed indole analogue-mediated increases in *GCLC* mRNA. In summary, the use of the indole analogues identified NADPH oxidase activity as a novel upstream activity regulating Nrf2/Keap1 signaling of *GCLC*, provided data supporting the hypothesis that Keap1 is a downstream effector for oxidase activity, and afforded *in vivo* data to support the hypothesis that Keap1 thiols can act as molecular sensors of reactive oxygen species. Finally, the comparative structure analysis suggests that 2-indol-3-yl-methylenequinuclidin-3-ols may represent a prototype for the development of novel chemopreventative agents able to activate Keap1/Nrf2 signaling.

INTRODUCTION

GSH[3] is an amino thiol that exhibits nucleophilic, antioxidant, and detoxification functions and is synthesized in all mammalian cells by the sequential action of two enzymes: GCL and GSH synthetase (1). GCL is a heterodimeric enzyme catalyzing the first and rate-limiting step, formation of γ-glutamylcysteine. Gclc is the catalytic subunit of GCL and Gclm is the regulatory subunit. Gclc contributes all of the enzymatic activity and is feedback inhibited by GSH. Association of Gclm with the catalytic subunit lowers the apparent K_m for the substrate glutamate while increasing the apparent K_i for GSH. Whereas the K_m for cysteine binding is independent of Gclm binding, cysteine availability can limit GCL activity. Plasma GSH, a consequence of GSH efflux from kidney and liver, is an important source for cysteine (1). Plasma GSH is transported into cells that express the enzyme γ-glutamyltranspeptidase as a γ-glutamyl amino acid and cysteinylglycine. Cysteinylglycine is broken down to cysteine and glycine by dipeptidase, a component of the γ-glutamyl cycle (1). Thus, GSH can act as a nucleophile, an antioxidant, and as a major storage form of the amino acid cysteine, the intracellular transport of which can enhance the rate of GSH synthesis (1).

GSH and its constituent amino acid, cysteine, are important components of cancer chemoprevention strategies. GCL is an integral component of phase II metabolism; induction of GCL and elevation of GSH synthesis occur rapidly after exposure to chemoprevention agents such as dithiolethiones (2). Increasing the intracellular concentration of cysteine or GSH has the potential to decrease arsenite-mediated induction of VEGF and hypoxia-inducible factor 1 in normoxic cells (3), arsenite-mediated genotoxicity (4), and tumor promotion and progression stimulated by 12-*O*-tetradecanoylphorbol-13-acetate (5, 6). These chemoprevention functions are a consequence of the chemical properties of the constituent sulfhydryl (reviewed in Ref. 7). The nucleophilic and reductive character helps to prevent metabolic activation of xenobiotics to mutagens and prevent reaction of mutagens with key cellular targets. The antioxidant attributes of GSH avert peroxide and superoxide-mediated genotoxicity. Thiol conjugation to mutagenic and carcinogenic xenobiotics and their subsequence efflux during phase II detoxification metabolism augment the chemopreventive properties of GSH.

The antitumor properties of NAC buttress the hypothesis that cysteine and GSH may act as chemopreventive agents. NAC is a prodrug that is deacetylated to L-cysteine, allowing increased GSH synthesis to occur. NAC can suppress benzo(*a*)pyrene-mediated tumor formation (8), inhibit expression of VEGF in Kaposi's sarcomas, and inhibit the growth of Kaposi's sarcomas in nude mice (9). NAC has also been shown to lower cancer-associated biomarkers in smokers (10).

Current strategies designed to elevate GSH concentrations involve using GSH esters or prodrugs such as NAC. It can be reasoned that prodrug strategies, which act by increasing intracellular cysteine, have the potential to be augmented by administration of compounds that induce expression of *GCLM* and/or *GCLC*. Recently, we made the novel observation that the nonsteroidal anti-inflammatory drug indomethacin induced Nrf2 (nuclear factor-erythroid 2p45-related transcription factor)-mediated expression of *GCLC* and *GCLM* in human hepatoma HepG2 cells (11). The indolic drug, indomethacin, is a 5-methoxy-2-methylindole-3-acetic acid analogue bearing an *N*-4-chlorobenzoyl substituent that exhibits unique multifunctional cancer chemopreventive activities, *e.g.*, tumor cell apoptosis and nonselective inhibition of prostaglandin synthesis (12). The observation that indomethacin also induces GSH synthesis suggests that various structural characteristics of this compound may be useful in designing novel multifunctional chemopreventive agents.

Indomethacin-mediated induction of *GCLC* and *GCLM* was shown to be regulated by Keap1-Nrf2 interactions (11). Nrf2 is a NF-E2-like

Received 3/28/03; revised 6/6/03; accepted 6/23/03.

The costs of publication of this article were defrayed in part by the payment of page charges. This article must therefore be hereby marked *advertisement* in accordance with 18 U.S.C. Section 1734 solely to indicate this fact.

[1] Supported in part by NIH Grants DK02603, CA91907, CA38079, and AA12600.

[2] To whom requests for reprints should be addressed, at Department of Radiation Oncology, B 902 TVC, Vanderbilt University School of Medicine, Nashville, TN 37232. E-mail: michael.freeman@vanderbilt.edu.

[3] The abbreviations used are: GSH, glutathione; GCL, glutamate cysteine ligase; IAA, iodoacetic acid; NAC, *N*-acetylcysteine; VEGF, vascular endothelial growth factor; MEF, mouse embyro fibroblast; 6FAM, 6-carboxyfluorescein; TAMRA, 6-carboxytetramethylrhodamine; DIGE, differential gel electrophoresis; ROS, reactive oxygen species; DPI, diphenyleneiodonium; SOD, superoxide dismutase; MRP, multidrug resistance-associated protein.

basic leucine zipper transcriptional activator and a member of the Cap 'n' Collar basic region leucine zipper family of transcription factors (13). Heterodimeric forms of Nrf2 bind to antioxidant response elements located in the proximal promoters of *GCLC* and *GCLM* (14). In unstressed cells, Nrf2 is tethered to the protein Keap1 (15). Keap1 is an actin-binding protein that resides in the cytosol and is a homologue of the *Drosophila* actin-binding protein Kelch. Tethering of Nrf2 by Keap1 requires that Keap1 form a homodimer, the formation of which is regulated by Ser^{104} (16). Homodimeric Keap1 tethers Nrf2 in the cytosol via association with the Neh2 domain of Nrf2 (15). Recent work performed *in vitro* with purified Keap1 supports the hypothesis that critical Keap1 cysteine residues may act as sensors of oxidative and electrophilic stress, regulating release of Nrf2 (17). It is not known whether Keap1 cysteines can react with oxidants and electrophiles *in vivo*.

Exposure to indomethacin causes Keap1 to release Nrf2 (11). The free Nrf2 translocates to the nucleus, induces transcription, and enhances translation of GCL. This is followed by elevation of GSH concentrations (11). Cells exposed to indomethacin are resistant to diethyl maleate-mediated GSH depletion and cytotoxicity. Exposure to antioxidants blocked indomethacin-mediated release of Nrf2 from Keap1, Nrf2 translocation, and transcription of *GCLC* (11).

The mechanism by which indomethacin activates Keap1 to release Nrf2 and induce *GCLC* is not currently known. The results obtained using antioxidants suggest that ROS are involved. As stated above, indomethacin exhibits several multifunctional chemopreventive activities. It is very likely that each of the activities of indomethacin is a consequence of specific molecular shapes. To elucidate the structural features that maximize Nrf2 activation, novel functionalized indoles and other structurally related compounds were synthesized and used along with indomethacin to conduct a comparative structure analysis. These experiments identified NADPH oxidase as a new upstream signaling activity capable of inducing Nrf2-mediated expression of *GCLC*, identified Keap1 as molecular target for NADPH oxidase activity, and provided novel *in vivo* data that are consistent with the hypothesis that thiol reactivity of Keap1 cysteines is an important component of regulation. Finally, these studies suggest that 2-indol-3-yl-methylenequinuclidin-3-ols may represent a prototype for the development of potentially novel chemopreventative agents for induction of *GCLC*.

MATERIALS AND METHODS

Indole Analogues and Related Compounds. The indole analogues and related compounds were prepared by aldol condensation of the appropriate *N*-substituted indole-3-, thiophene-3-, or phenylcarboxaldehyde with 1-aza-bicyclo[2.2.2]octan-3-one to afford the corresponding arlymethylene-1-aza-bicyclo[2.2.2]octan-3-one derivative. These 3-keto analogues were also reduced to the corresponding (±)-1-aza-bicyclo[2.2.2]octan-3-ol analogue with sodium borohydride in methanol. Confirmation of structure and purity of these analogues was obtained from ^{1}H NMR and ^{13}C NMR spectroscopic analysis and from carbon, hydrogen and nitrogen combustion analysis. The geometry of the double bond in these molecules was established from X-ray crystallographic data.[4]

Cell Culture and DNA plasmids. HepG2 cells were maintained in DMEM supplemented with 10% fetal bovine serum, 1% sodium pyruvate, and 20 μg/ml gentamicin. MEFs were maintained in DMEM:Ham's F-12 supplemented with 15% fetal bovine serum and 100 μM β-mercaptoethanol. The cDNA *KIAA0132* (human Keap1) was a gift from Dr. Takahiro Nagase and was subcloned into pCMV-Tag (Stratagene). The vector pCMV-Tag places a FLAG epitope NH_2 terminus to Keap1. A human *GCLC* promoter fragment was cloned from a human bacterial artificial chromosome library and subcloned into pGL3Basic (Promega). The full-length fragment encompasses bp −3678 to +246, with +1 representing the transcriptional start site. All constructs were verified by sequencing.

Transfections. Cells were inoculated into either T-25 flasks (3×10^5) or 6-well dishes (2×10^5) 15 h before transfection. Plasmids were transiently transfected into cells using DMRIE-C (Invitrogen). After transfection, cells were serum starved overnight and then exposed to the indoles. β-Galactosidase and luciferase activities were determined using a Promega Reporter Assay System according to the manufacturer's directions. Briefly, cells were lysed in Reporter Lysis Buffer, vortexed, frozen, thawed, and centrifuged at $13{,}000 \times g$ for 3 min at 4°C. The supernatant was then recovered. For β-galactosidase activity, 100 μl of lysate were mixed with assay buffer (200 μl) and incubated at 37°C for 3 h, and the reaction was stopped upon addition of sodium carbonate. The absorbance at 420 nm was then determined. For determination of luciferase activity, 10 μl of lysate were mixed with 100 μl of luciferase assay reagent and placed in a luminometer. All experiments involving reporter assays were done in triplicate and repeated at least twice.

Generation of HepG2 Cells That Stably Overexpress Either FLAG/Keap1, FLAG/Luciferase, or pcDNA 3.1. Cells were transfected with 1 μg of plasmid [pCMV-Tag/Keap1, pCMV-Tag/luciferase (Stratagene), or pcDNA3.1 (Invitrogen)] and selected for resistance to 1000 μg/ml G418. Individual clones were isolated and expanded. Cells were maintained in 500 μg/ml G418. However, G418 was omitted from the culture medium during experimental manipulations. Cell lines stably transfected with pCMV-Tag/Keap1 were labeled as HepG2/Keap1/J1, HepG2/Keap1/J2, and HepG2/Keap1/J3. Cell lines stably transfected with pCMV-Tag/luciferase were labeled as HepG2/Lux/S6 and HepG2/Lux/S7. Cell lines stably transfected with pcDNA3.1 were pooled and labeled as HepG2/pc.

Northern Blot Analysis. Total RNA was isolated using Trizol reagent (Invitrogen). The isolated RNA (20 μg/lane) and a RNA ladder were fractionated by electrophoresis in a 1.1% agarose/2.2 M formaldehyde gel, blotted onto nitrocellulose membranes, and baked. Prehybridization and hybridization were carried out at 42°C using ^{32}P-labeled cDNA corresponding to *GCLC* or cyclophilin. All experiments were repeated two or more times.

Immunoblot Analysis. The cells were treated as indicated, lysed at intervals using NP40 lysis buffer [50 mM Tris-Cl (pH 7.8), 150 mM NaCl, 1% NP40, 10 mM EDTA, and 10 mg/ml protease inhibitor mixture (Sigma)], briefly sonicated, and incubated in ice for 30 min. Lysates were clarified by centrifugation (12,000 rpm for 5 min), and 30 μg of lysates were resolved on 10% SDS-polyacrylamide gels and transferred to nitrocellulose membranes for 1 h. Membranes were incubated overnight with antibody. Membranes were developed by the enhanced chemiluminescence system (Amersham Pharmacia Biotech).

Real-Time Quantitative Reverse Transcription-PCR. Total RNA was isolated using Trizol reagent and treated with DNase I before performing reverse transcription. Two μg of total RNA were reverse transcribed using mouse *GCLC* and mouse cyclophilin, coamplified as an internal control. The reverse primers were mGCLC (GGTGTCTATGCTCATCAGGGTG) and mCyclophilin (GGCGTGTAA AGTCACCACCC). The cDNA products underwent PCR amplification using GCLC and mCyclophilin forward primers (5′ to 3′) mGCLC (GGTGCAGCAAGGCCCA) and mCyclophilin (TCGAGCTCTGAGCACTGGAG) and reverse primers (5′ to 3′) mGCLC (GGTGTCTAT GCTCATCAGGGTG) and mCyclophilin (GGCGTGTAAAGTCACCACCC) plus TaqMan probes labeled with 5′ fluorescent label, 6FAM, and 3′ Quencher TAMRA (Applied Biosystems). The sequence of the GCLC probe (5′ to 3′) was 6FAM-GCAGCTCTGAGCCAGCTGCAGAGG-TAMRA. The sequence of the cyclophilin probe (5′ to 3′) was 6FAM-AGCAGCTCTGAGCCAGTCGACGAGG-TAMRA. Real-time quantitative PCR was performed and analyzed using an ABI PRISM 7700 Sequence Detector.

Determination of Keap1 Thiol Reactivity and Isoelectric Focusing. Thiol reactivity was assessed using a modification of the method described in Ref. 18. Cells were transiently transfected with the FLAG/Keap1 vector (1 μg/flask). Cells were then labeled with [^{35}S]methionine in methionine-free medium, washed, and exposed to experimental manipulation. For immunoprecipitation, cells were washed twice in ice-cold PBS and solubilized in 0.01%Triton X-100, 0.5% sodium deoxycholate, and 0.1% SDS plus protease inhibitor mixture (P1860; Sigma). Solubilized protein was immunoprecipitated with anti-FLAG antibody (Sigma)/protein G/A (Oncogene) and then washed

[4] P. A. Crooks and V. N. Sonar, unpublished data.

three times with solubilization buffer. IAA was dissolved in 300 mM Tris (pH 8.5) and added to urea buffer [21 mM 4-morpholinepropanesulfonic acid, 9.5 mM urea, and 2% NP40 (pH 8.5)] so that the final IAA concentration was 50 mM. Thirty μl of the IAA/urea buffer were added to the washed pellet. A 10-cm slab gel isoelectric focusing gel (9.2 M urea, 4% acrylamide, 2% NP40, and 3.75% 3–10 ampholines) was prefocused at 25.5°C for 105 min (cathode, 0.02 M sodium hydroxide; anode, 0.01 M phosphoric acid) before the addition of immunoprecipitated, IAA *S*-alkylated sample. Isoelectric focusing was performed at 25.5°C using 240 V for 18 h. The gel was then fixed, exposed to En3Hance (DuPont), dried, and subjected to fluorography.

Two-dimensional DIGE. DMSO (control) and indomethacin-treated FLAG/Keap1 immunocomplexes were precipitated as described. Immunoprecipitates were precipitated with 4 volumes of methanol and 1 volume of $CHCl_3$ and resuspended in two-dimensional DIGE lysis buffer (7 M urea, 2 M thiourea, 4% 3-[(3-cholamidopropyl)dimethylammonio]-1-propanesulfonic acid, 5 mM MgOAc, and 30 mM Tris) and labeled with 200 pmol of Cy3 (DMSO) or Cy5 (indomethacin treated) for 30 min on ice. The labeling reaction was quenched with 1 μl of 10 mM lysine, combined and mixed with an equal volume of rehydration buffer [7 M urea, 2 M thiourea, 4% 3-[(3-cholamidopropyl)dimethylammonio]-1-propanesulfonic acid, 2% DTT, 0.5% IPG buffer (pH 3–10NL)]. The mixed Cy3/Cy5-labeled sample was used to rehydrate a 24-cm pH 3–10 nonlinear immobilized pH gradient strip, which was subsequently focused for 82,000 volt hours using an IPGphor isoelectric focusing unit (Amersham Biosciences). The second-dimension SDS-PAGE separation was carried out on a continuous 12.5% polyacrylamide gel. The Cy3- and Cy5-labeled proteins were individually imaged from the intact two-dimensional gel using a Perkin-Elmer Two-dimensional Master Gel Imager at 100 μM resolution, using excitation and emission wavelengths that were mutually exclusive for each dye. Cy3-labeled proteins were imaged for 15 s using 540 and 590 nm for excitation and emission wavelengths, respectively; Cy5-labeled proteins were imaged for 12 s using 620 and 680 nm for excitation and emission wavelengths, respectively. Sixteen-bit tagged image file format files were used to determine the Cy3:Cy5 volume ratios for each isoform using DeCyder software (Amersham Biosciences).

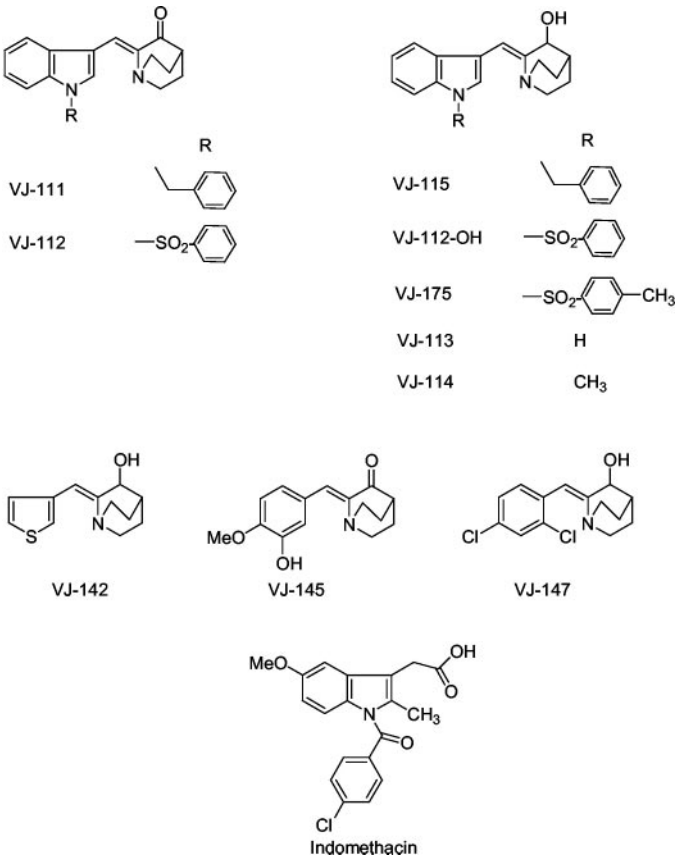

Fig. 1. The structures of indomethacin, a series of novel indole analogues, and structurally related compounds.

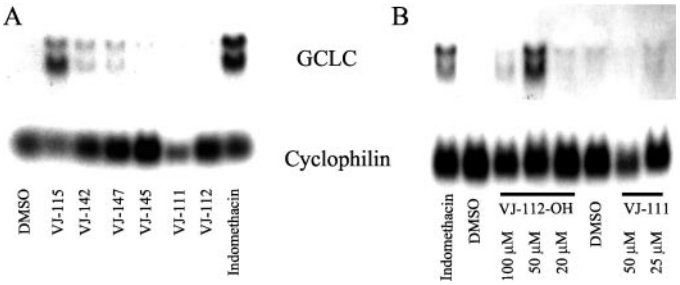

Fig. 2. Northern blot illustrating expression of *GCLC* mRNA isolated from exposure of HepG2 cells to indole analogues or structurally related compounds for 18 h. *A*, cells were exposed to vehicle control (DMSO), 50 μM of the indicated synthetic analogue, or 500 μM indomethacin. *B*, cells were exposed to DMSO; 500 μM indomethacin; 20, 50, or 100 μM VJ-112-OH; or 25 or 50 μM VJ-111.

Determination of NADPH Oxidase Activity. Cell membranes were isolated by differential centrifugation according to the method of Mohazzab and Wolin (19). In brief, cells from six 75% confluent T-75 flasks were harvested with cell dissociation solution (PBS-EDTA), washed once with ice-cold Dulbecco's PBS, and centrifuged for 5 min at 700 $\times$ *g*. Supernatant was discarded, and the pellet was resuspended in 2.5 ml of ice-cold Tris-sucrose buffer [pH 7.1; composed of 10 mM Trizma base, 340 mM sucrose, 1 mM EDTA, and 10 μg/ml protease inhibitor mixture (Sigma)] and sonicated by four 15-s bursts. The cellular homogenate was clarified by centrifugation at 1,475 $\times$ *g* at 4°C for 15 min to remove nuclei and unbroken cells. The supernatant was then centrifuged at 30,000 $\times$ *g* at 4°C for 30 min. The pellet was discarded, and the supernatant was further centrifuged at 100,000 $\times$ *g* at 4°C for 75 min. The pellet was resuspended in 150 μl of Tris-sucrose buffer and stored at −80°C. Generation of ROS was measured by chemiluminescence as follows: in a 500-μl reaction buffer [50 mM phosphate buffer (pH 7.0), 1 mM EGTA, 150 mM sucrose, 5 μM lucigenin], 15 μg of cell membrane protein and 100 μM NADPH as substrate were added and incubated at 37°C for 5 min. In some experiments, DPI or SOD was added in the reaction mixture. Chemiluminescence (in arbitrary light units) was measured by using a Monolight 3010 luminometer (BD PharMingen) for 10 s. The signal was expressed as the sum of all measurements after subtraction of the buffer blank.

Measurement of MRP Activity. Cells were labeled with 10 μg/ml C-369 (carboxy-2′,7′-dichlorofluorescein; Molecular Probes) dissolved in DMSO at 37°C for 15 min, placed immediately on ice, and analyzed by flow cytometry (excitation, 488 nm; emission, 525 nm). Mean fluorescence intensity of 20,000 cells was calculated from the histograms obtained from each sample and corrected for autofluorescence obtained from unlabeled samples.

RESULTS

To elucidate the molecular targets that are critical for induction of *GCLC* by indole analogues, a series of novel 2-indol-3-yl-methylenequinuclidine analogues and some related compounds were synthesized (Fig. 1), and a comparative structure analysis was conducted. The data presented in Fig. 2 illustrate two representative Northern blots, whereas the data presented in Table 1 summarize the results from these and other experiments. It is immediately evident that of the 10 synthetic analogues evaluated, 2-indol-3-yl-methylenequinuclidin-3-ols containing either an indolic *N*-benzyl or *N*-benzenesulfonyl substituent constitute the most potent inducers of *GCLC* mRNA. Oxidation of the quinuclidine 3-hydroxy group to a 3-keto group results in complete loss of activity, and substitution of the indolic *N*-aromatic substituent with a methyl group or a hydrogen atom also affords inactive compounds. In addition, substitution of the indol-3-yl moiety with a thiophen-3-yl or substituted phenyl moiety decreases activity by approximately 85% (Table 1). This structure-activity profile is interesting because the three most active compounds have some structural characteristics that are found in the structure of indomethacin, *i.e.*, all four molecules contain an indol-3-yl moiety bearing an aromatic *N*-substituent in their structures.

Table 1 *Northern blot analysis of GCLC expression*

HepG2 cells were exposed to the indicated compounds (50 μM) for 18 hr, and then RNA was isolated.

Compound	Relative expression of *GCLC*[a]
VJ-115	50
VJ-112-OH	50
VJ-175	50
VJ-142	8
VJ-147	7
VJ-145	1
VJ-111	1
VJ-112	1
VJ-113	1
VJ-114	1

[a] *GCLC* and cyclophilin mRNA levels were determined by Northern blotting and quantitated using image analysis software. *GCLC* levels in treated cells were divided by cyclophilin levels and expressed relative that obtained from DMSO-exposed controls.

Elevation of *GCLC* mRNA was accompanied by elevation in intracellular GSH concentrations. Previous work established that GSH concentrations increased after *GCLC* mRNA induction mediated by exposure to indomethacin (11). Similar results were obtained when cells were exposed to an indole analogue. Cells were exposed to the indole analogue VJ-175 for 18 h, and then intracellular GSH was measured as described in Ref. 11. Cells exposed to vehicle control (DMSO) contained 30 $\pm$ 5 nmol GSH/mg protein (n = 4), whereas cells exposed to VJ-175 contained 78 $\pm$ 13 nmol GSH/mg (n = 4). These results indicate that the increase in *GCLC* mRNA observed after exposure to an indole analogue such as VJ-175 (Fig. 9) is accompanied by elevation of GSH.

Two approaches were used to evaluate the role of Nrf2 in indole analogue-mediated signaling. First, quantitative assessment of *GCLC* mRNA levels in MEFs obtained from wild-type and Nrf2-null animals was performed using real-time PCR (Fig. 3*A*). The data shown in Fig. 3*A* indicate that exposure of wild-type MEF cells to various concentrations of VJ-112-OH resulted in an elevation of *GCLC* mRNA, whereas *GCLC* mRNA was not increased in Nrf2-null cells. Thus, loss of Nrf2 expression abrogated *GCLC* gene expression mediated by exposure to an indole analogue.

In a second approach, HepG2 cells were stably transfected with a vector that expressed FLAG-tagged Keap1, and various clones were isolated. In addition, control cell lines that were stably transfected with either FLAG-tagged luciferase or pcDNA3.1 were generated. Expression of luciferase in control cell lines was verified by luminometry (data not shown). Keap1 is an actin-binding protein, and under basal conditions it sequesters Nrf2 in the cytosol (15). In unstressed HepG2 cells, Nrf2 can be observed in the cytosol and in the nucleus (20), suggesting that Nrf2 synthesis exceeds that of Keap1. Therefore, overexpression of Keap1 would be expected to suppress Nrf2-mediated gene expression. The expression of FLAG/Keap1 in three individual clones that overexpress Keap1 is illustrated in the immunoblot shown in Fig. 3*B*. The three clones that overexpress FLAG/Keap1 and pooled control HepG2/pc cell lines were transiently cotransfected with pGL3/GCLC and pcDNA3.1/LacZ. The pGL3/*GCLC* reporter vector expresses luciferase under control of the human *GCLC* proximal promoter and is Nrf2 dependent (11). Luciferase activity, corrected for β-galactosidase activity (a measure of transfection efficiency), was significantly diminished in cells that overexpress Keap1 compared with the parental control cells ($P \leq 0.05$, ANOVA). These results are consistent with previous work indicating that human *GCLC* was regulated by Nrf2 activity (14).

MRPs are drug efflux pumps that belong to the phase II metabolic gene family (21), and Nrf2 has been shown to regulate expression of

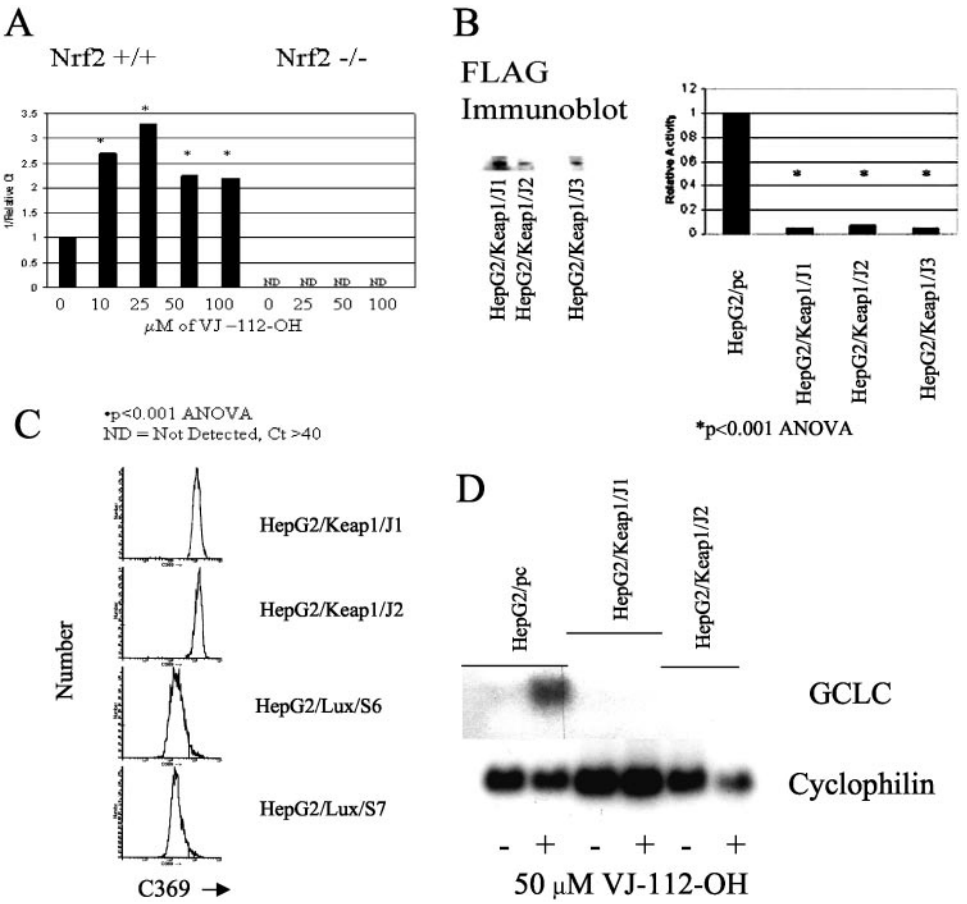

Fig. 3. Indole analogue-mediated elevation of *GCLC* mRNA is inhibited in Nrf2-null MEF cells or in cells that overexpress Keap1. *A*, MEF cells derived from wild-type or Nrf2-null mice were exposed to various concentrations of VJ-112-OH, and then RNA was isolated. *GCLC* mRNA was quantitated by real-time reverse transcription-PCR. The relationship between cycle threshold (Ct) and *GCLC* mRNA levels was corrected for changes in expression of cyclophilin mRNA. *B*, HepG2 cells that stably express pcDNA3.1 (HepG2/pc) or FLAG/Keap1(HepG2/Keap1/J1, HepG2/Keap1/J2, HepG2/Keap1/J3) were transiently cotransfected with 0.1 μg of pGL3/GCLC and 0.5 μg of pcDNA3.1/LacZ. An immunoblot demonstrating expression of FLAG/Keap1 is shown to the *left* of the histogram. *C*, histogram illustrating MRP activity measured by flow cytometric analysis of control cells (HepG2/Lux/S6 and HepG2/Lux/S7) or cells overexpressing Keap1 (HepG2/Keap1/J1 and HepG2/Keap1/J2) labeled with the fluorescent dye C-369. *D*, Northern blot of *GCLC* and cyclophilin mRNA from HepG2 cells, HepG2/Keap1/J1, or HepG2/Keap1/J2 cells. Cells were exposed to 0 or 50 μM VJ-112-OH for 18 h.

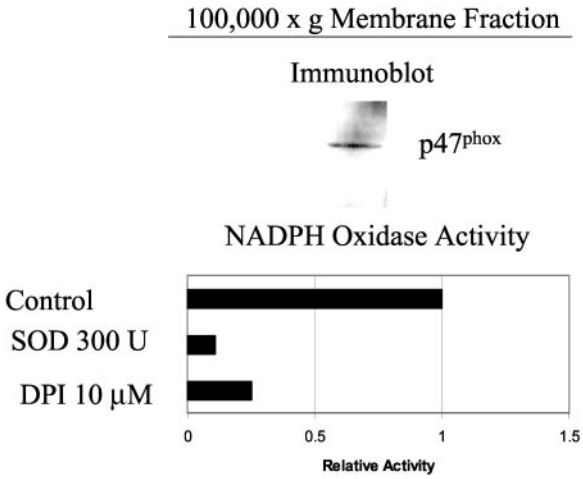

Fig. 4. NADPH oxidase activity in HepG2 membrane fractions. Membranes isolated after centrifugation at 100,000 × *g* were either immunoblotted for the presence of $p47^{phox}$ or used to measure the activity of the NADPH oxidase. In some membrane fractions, SOD or DPI was added before activity measurements.

this family, as discussed in Ref. 22. We used a flow cytometric analysis technique (23) to determine whether overexpression of Keap1 affected MRP activity. Fig. 3*C* illustrates the fluorescent intensity of the anionic dye C-369 (Molecular Probes) obtained from control cell lines that stably express FLAG/luciferase (HepG2/Lux/S6 and HepG2/Lux/S7) and from cell lines that overexpress Keap1 (HepG2/Keap1/J1 and HepG2/Keap/J2). Cell lines that overexpressed Keap1 exhibited enhanced accumulation of dye compared with control cell lines, indicating loss of MRP efflux activity. These results are consistent with the expectation that overexpression of Keap1 will down-regulate Nrf2-mediated gene expression.

The pooled control of HepG2/pc cells and two clones that overexpress FLAG/Keap1 were exposed to the indole analogue VJ-112-OH. RNA was isolated and subjected to Northern blotting (Fig. 3*D*). The data indicate that exposure to VJ-112-OH increased *GCLC* mRNA levels in control cells, but not in cells that overexpress Keap1. Thus, the results obtained using Nrf2-null MEFs and Keap1-overexpressing cell lines, combined with previous data obtained using indomethacin (11), indicate that Nrf2/Keap1 signaling regulates indole-mediated *GCLC* gene expression.

The observations that the antioxidant NAC blocked indomethacin-mediated release of Nrf2 from Keap1, Nrf2 translocation, and transcription of *GCLC* (11) suggested that ROS signaling may be essential for induction of *GCLC* by the indole indomethacin. Indomethacin is known to increase the activity of the ROS-generating enzyme NADPH oxidase (24). This multisubunit enzyme is composed of a membrane flavocytochrome b_{558} complex consisting of a Nox/Duox family member and $gp22^{phox}$ and several cytosolic subunits [Rac, $p67^{phox}$, $p47^{phox}$, and $p40^{phox}$ (25, 26)]. The activated enzyme complex requires translocation of cytosolic subunits to the membrane so that it may catalyze the one-electron reduction of oxygen to superoxide anion using NADPH as a substrate. HepG2 cells have been shown to express the Nox1 homologue (27).

As shown in Fig. 4, HepG2 cells express NADPH oxidase activity. A 100,000 × *g* membrane fraction was isolated and used for immunoblotting and determination of oxidase activity. Immunoblot analysis indicated the presence of the $p47^{phox}$ subunit in the membrane fraction. This is consistent with the observation that membrane fractions exhibit NADPH-dependent superoxide production [assessed by lucigenin chemiluminescence (28)] that could be inhibited by either SOD or DPI, an inhibitor of cytochrome b_{558}, the flavocytochrome subunit of the oxidase (Fig. 4).

Exposure of HepG2 cells to the indole analogue VJ-115 for up to 5 h increased NADPH oxidase activity (Fig. 5). After exposure to the analogue, a 100,000 × *g* membrane fraction was isolated, and activity was measured. The data were best fitted by a straight line ($r = 0.994$). This result is consistent with the work of Tanaka *et al.* (24), who observed a linear increase in indomethacin-mediated activation of NADPH oxidase activity in leukocytes as a function of time exposure. This work is also consistent with our previous work (11), which demonstrated that indole exposure increased intracellular levels of ROS in a linear fashion as a function of time of exposure.

It has been hypothesized that Keap1 cysteine residues act as molecular sensors of electrophilic molecules or ROS (15, 29). Using an *in vitro* assay, Dinkova-Kostova *et al.* (17) have shown that mouse Keap1 thiol moieties can react with electrophilic molecules such as dexamethasone mesylate and release Nrf2.

Human Keap1 contains 27 cysteine residues. The thiol reactivity of Keap1 cysteines was assessed in cells treated with the indole indomethacin using a modification of the method described by Thomas and Beidler (18). This technique uses IAA to *S*-alkylate reduced thiols of cysteine and analyzes the results by isoelectric focusing. IAA will not react with a thiol residue that is not reduced. For example, it will not react with oxidized thiols. IAA *S*-alkylation of cysteines introduces a negative charge on the residue. During isoelectric focusing, proteins with the greatest number of IAA *S*-alkylations (a function of the number of reduced thiols available for reaction with IAA) will focus closer to the anode compared with those that have fewer *S*-alkylations.

Keap1 is extremely amenable to this analysis. The pI of FLAG/Keap1 was calculated using ExPASy pI software and predicted to be 5.81 (no alkylations). Alkylation of a single FLAG/Keap1 cysteine would decrease the pI to a value of 5.75, two alkylations would decrease the pI to 5.69, and alkylation of all cysteine residues would result in the protein exhibiting a pI of 4.81. As a comparison, the predicted pI of Nrf2 is 4.67. Complete alkylation of all cysteine residues in Nrf2 would decrease the pI to 4.60. This calculation for Nrf2 indicates that it would not be a good candidate for this type of analysis because there would be very little change in pI.

Two-dimensional DIGE (Amersham Biosciences) was used to assess the degree of IAA *S*-alkylation. Cells were transfected with FLAG/Keap1 and exposed to DMSO or indomethacin (500 µM/2 h; Fig. 6). FLAG/Keap1 was immunoprecipitated, alkylated with IAA (50 mM), and then labeled with either Cy3 (DMSO treated) or Cy5 (indomethacin treated) fluorescent dyes. Control and indomethacin-treated samples were combined together and run on a single two-dimensional gel. Although the Cy3-labeled Keap1 isoforms and the Cy5-labeled Keap1 isoforms focused at the same pIs and exhibited the

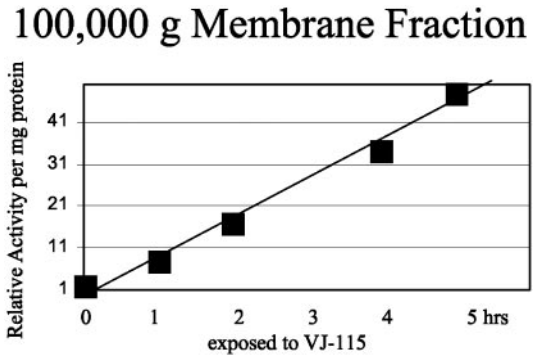

Fig. 5. NADPH oxidase activity increases in HepG2 cells exposed to 50 µM VJ-115. Cells were exposed to VJ-115 for the indicated times, and then 100,000 × *g* membrane fractions were isolated and used for determination of oxidase activity. Activity is expressed relative to that measured in untreated cells.

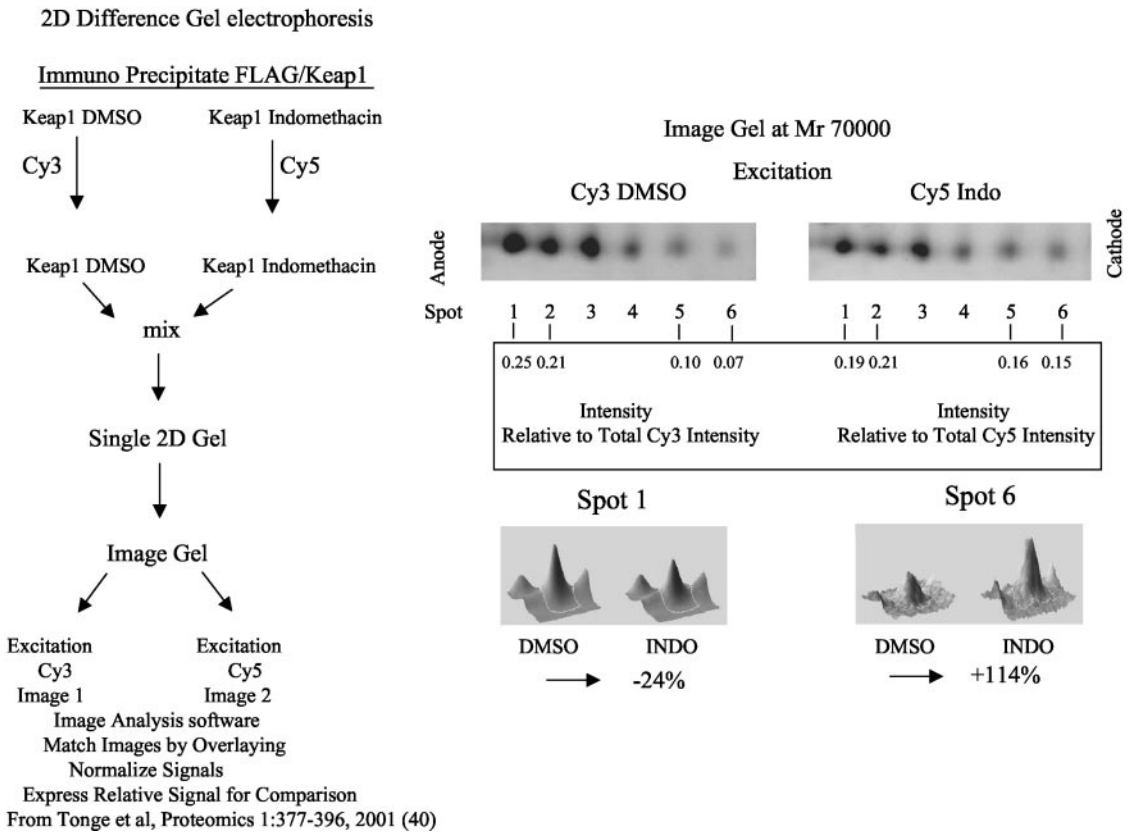

Fig. 6. Analysis of FLAG/Keap1 treated with indomethacin using two-dimensional DIGE. HepG2 cells were transiently transfected with 1 μg of FLAG/Keap1 per T-25 flask and then exposed to either DMSO or indomethacin (500 μM/2 h). FLAG/Keap1 was immunoprecipitated and *S*-alkylated with 50 mM IAA. The immunocomplexes were then subjected to two-dimensional difference gel electrophoresis using Cy3 and Cy5 fluorescent dyes to prelabel the protein samples before separation on the same two-dimensional gel (42). Shown are the Cy3 and Cy5 specific images obtained from the same isoforms from the M_r ~70,000 region of the two-dimensional gel. Quantitative fluorescent images of the Cy3 (DMSO)- and Cy5 (indomethacin)-labeled samples were normalized and compared for Cy3:Cy5 volume ratios as indicated. Three-dimensional contours are shown for representative volume comparisons using the Cy3 and Cy5 dyes, which exhibit a linear dynamic range over 4 orders of magnitude.

same molecular weight (M_r 70,000, the estimated molecular weight for FLAG/Keap1), the proteins could be imaged separately using excitation and emission wavelengths that are mutually exclusive for the two dyes. These dyes exhibit a linear dynamic range of over 4 orders of magnitude, allowing for quantitative comparison of abundance changes for the same protein spots resolved on the same two-dimensional gel. The two-dimensional DIGE analysis indicated a series of FLAG immunoreactive proteins differing in isoelectric point, all of which exhibited an apparent molecular weight of 70,000 (Fig. 6). Quantitative comparison of the volume ratios of the Cy3- and Cy5-labeled components present in each isoform was performed. The isoform represented by spot 1 exhibits a molecular weight of 70,000 that focused closest to the anode and thus underwent the greatest number of *S*-alkylation events. The isoform represented by spot 6 represents a FLAG immunoreactive protein that exhibits a molecular weight of 70,000 that focused closest to the cathode. It underwent the least number of IAA mediated *S*-alkylations. The Cy3 intensity in each spot was determined and summed for all six spots (ΣI_{1-6}). The Cy3 intensity of a spot is shown relative to the sum of the Cy3 intensities measured in all six spots (*e.g.*, $\Sigma I_1/\Sigma I_{1-6}$). A similar calculation was made for Cy5. Exposure to indomethacin resulted in a 24% decrease in the relative intensity of spot 1, whereas the relative intensity of spot 6 increased 114%. The indomethacin-mediated loss of IAA reactivity is statistically significant compared with control ($P \leq 0.05$, paired Student's *t* test). This shift is also illustrated as three-dimensional images. The indomethacin-mediated changes in IAA *S*-alkylation were interpreted to indicate that exposure to an indole analogue caused a change in the thiol oxidation states of Keap1 cysteine residues.

Slab gel isoelectric focusing was also used to assess IAA *S*-alkylation of Keap1. HepG2 cells were again transiently transfected with FLAG-tagged Keap1. Cells were then labeled overnight with [^{35}S]methionine and exposed to DMSO (control) or indomethacin (500 μM) for 2 h, and then FLAG/Keap1 was immunoprecipitated using FLAG antibody. An aliquot of the immunoprecipitated FLAG/Keap1 was subjected to one-dimensional PAGE/fluorography (Fig. 7*A*), and a second aliquot was subjected to immunoblotting (Fig. 7*B*). The fluorograph (a 24-h exposure) shown in Fig. 7*A* indicates the presence of two immunoprecipitated bands in control and indomethacin-treated samples. The faster migrating band has a molecular weight of approximately 70,000 (the estimated molecular weight for FLAG/Keap1). The immunoblot (exposure time of 30 s) indicates the presence of two immunoprecipitated bands in control and indomethacin-treated samples (Fig. 7*B*). The faster migrating band has a molecular weight of approximately 70,000. The slower migrating band had a molecular weight of about 140,000. The immunoblot data suggest that the two bands shown in the fluorograph represent a FLAG/Keap1 monomer and a dimer of Keap1, which most likely formed during electrophoresis.

Next, cells were transfected with FLAG/Keap1, labeled with [^{35}S]methionine, and exposed to indomethacin (500 μM/2 h) or DPI (20 μM) plus indomethacin (500 μM /2 h; Fig. 8). FLAG/Keap1 was immunoprecipitated, alkylated with IAA (50 mM), and analyzed by isoelectric focusing/fluorography (Fig. 8*A*). Three lanes are shown

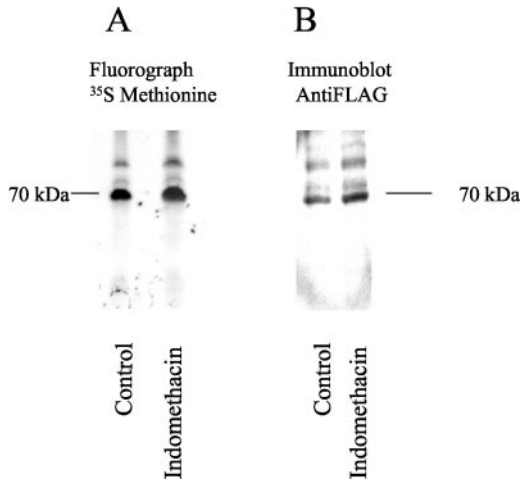

Fig. 7. Fluorograph and immunoblot of immunoprecipitated FLAG/Keap1. HepG2 cells were transiently transfected with 1μg of FLAG/Keap1 per T-25 flask, labeled with [^{35}S]methionine overnight, washed, and exposed to DMSO or 500 μM indomethacin for 2 h. Cells were solubilized, and FLAG/Keap1 was immunoprecipitated. The immunoprecipitated protein was subjected to one-dimensional PAGE fluorography and exposed to film for 24 h (*A*) or immunoblotted with anti-FLAG antibody (*B*; exposure time, 30 s).

(*Control*, *Indomethacin*, and *DPI + Indomethacin*), and each lane contains several bands. Band 1 focused nearest the anode, thus it was highly alkylated. Bands 2 and 3 focused closer to the cathode and thus represent protein that did not undergo extensive *S*-alkylation by IAA. These results can be reasonably interpreted to indicate the presence of several oxidation states for Keap1.

The isoelectric focusing analysis (Fig. 8*A*) indicated that exposure to indomethacin affected the oxidation states of Keap1 thiols, as assessed by the loss of IAA reactivity. This was determined as follows. The intensities of bands 1–3 and bands a and b were determined using image analysis software. Rectangles were drawn around each band, and the intensity within the rectangle was determined. The intensity of band 1 was expressed relative to the sum of the total intensities (band 1 + band 2 + band 3 + band a + band b) of a particular lane. A similar calculation was made for bands 2 and 3 (Fig. 8*B*). Band 1 focused closest to the anode, thus it represents Keap1 molecules containing the greatest number of reactive thiols. Bands 2 and 3 focused near the cathode, thus these bands represent Keap1 molecules with fewer reactive thiols. In the lane representing control cells, band 1 exhibited a relative intensity of approximately 50%. Bands 2 and 3 each composed less than 10% of the total. This was interpreted to indicate that in control cells, the majority of Keap1 molecules were in a reduced state and thus reactive to IAA. In the lane representing indomethacin-treated cells, the intensity of band 1 was diminished, and the intensity of band 2 was increased. Under these conditions, band 2 represented approximately 25% of the total intensity of that lane, whereas band 1 represented 35%. Compared with control, these changes were statistically significant ($P \leq 0.05$, Student's *t* test). These changes were interpreted to indicate an indole-mediated shift in the thiol oxidation states of Keap1. If cells were exposed to DPI (20 μM) for 1 h before and during the indomethacin treatment, the intensity of the Keap1 bands remained similar to control. This was interpreted to indicate that loss of NADPH oxidase activity blocked a change in Keap1 thiol reactivity.

HepG2 cells were exposed to various indoles analogues and structurally related compounds in the absence or presence of DPI, an inhibitor of cytochrome b_{558}, the flavocytochrome subunit of NAPDH oxidase (Fig. 9*A*). Exposure to indole analogues VJ-115, VJ-112-OH, or indomethacin in the absence of DPI produced a robust increase in *GCLC* mRNA. However, exposure to DPI before and during indole analogue exposure inhibited indole analogue-mediated induction of *GCLC* expression (Fig. 9*A*, compare *Lane 3* with *Lane 5*, *Lane 4* with *Lane 6*, and *Lane 11* with *Lane 12*). Similarly, exposure of cells to the proline-arginine-rich peptide PR-39 (30), which binds to and inhibits the p47^{phox} subunit of the oxidase, blocked VJ-175-mediated induction of *GCLC* (Fig. 9*B*). These results indicate that indole-mediated induction of *GCLC* was inhibited if the cytochrome b_{558} activity was inhibited, or if the p47^{phox} subunit of the oxidase was inhibited.

The indole analogue VJ-111 was unable to induce Nrf2-mediated expression of *GCLC* (Figs. 2 and 9). VJ-111 contains a quinuclidin-3-one group rather than the quinulidin-3-ol group found in VJ-115 or VJ-112-OH (Fig. 1). Thus, replacement of the 3-hydroxyl substituent in VJ-115 with a 3-keto group blocked gene induction. In addition, VJ-111 was unable to stimulate NADPH oxidase activity (data not

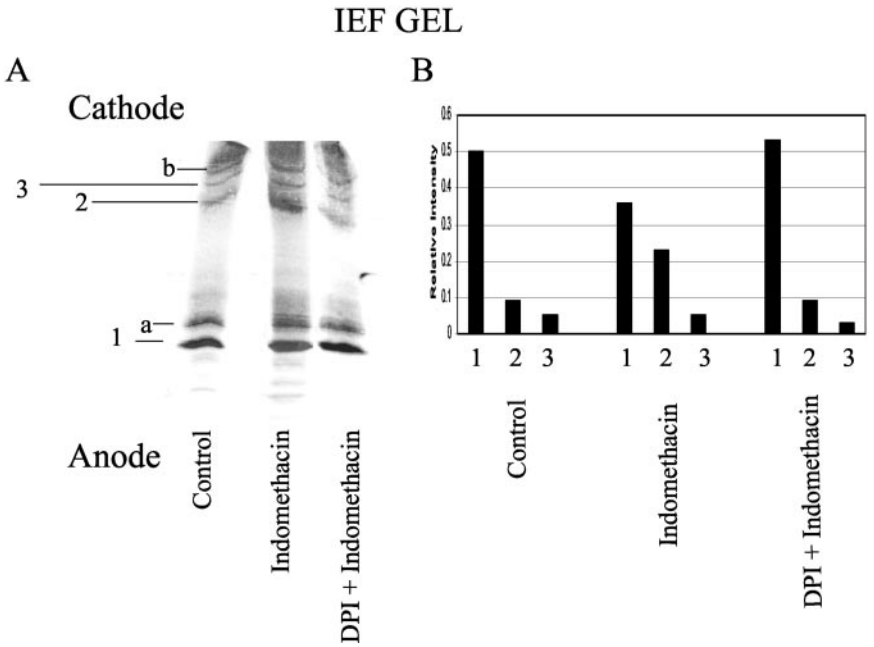

Fig. 8. Isoelectric focusing gel analysis of [^{35}S]methionine-labeled FLAG/Keap1. *A*, HepG2 cells were transiently transfected with 1μg of FLAG/Keap1 per T-25 flask, labeled with [^{35}S]methionine overnight, washed, and exposed to DMSO or 500 μM indomethacin for 2 h or DPI (20 μM) for 1 h, and then indomethacin (500 μM) was added to the cells, which were incubated for an additional 2 h. Cells were solubilized, and FLAG/Keap1 was immunoprecipitated. Immunoprecipitated protein was *S*-alkylated with IAA (50 mM) and analyzed by isoelectric focusing. *B*, image analysis software was used to measure the intensity of bands 1–3 and bands a and b as described in the text.

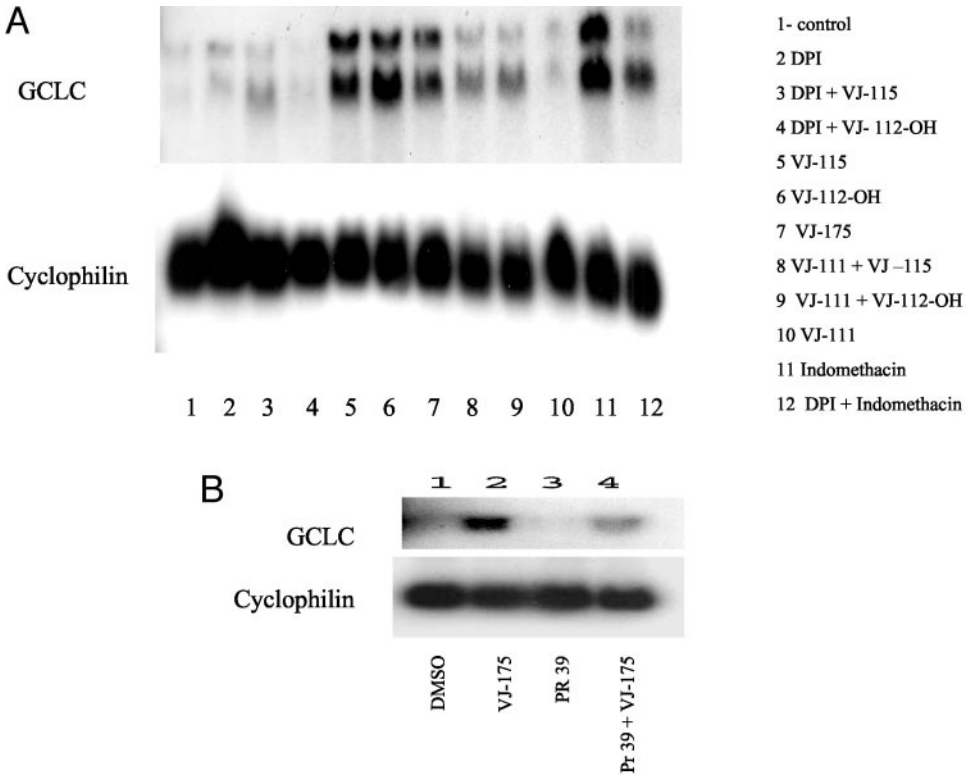

Fig. 9. *A*, Northern blot of *GCLC* mRNA. HepG2 cells were exposed to 0 or 10 μM DPI for 1 h. Then the indicated synthetic analogue (50 μM) or indomethacin (500 μM) was added, and the cells were exposed for an additional 17 h. *B*, Northern blot of *GCLC* mRNA. HepG2 cells were exposed to 0 or 10 μg/ml PR-39 peptide for 2 h before the addition of 0 or 50 μM VJ-175. Cells were exposed to the indole analogue for 18 h.

shown). If the indole analogues acted by stimulating NADPH oxidase, it is likely that compounds such as VJ-111 would inhibit *GCLC* induction by other indole analogues due to competition for key sites. Exposure to VJ-111 before and during exposure to VJ-115 or VJ-112-OH blocked indole analogue-mediated induction of *GCLC* (Fig. 9*A*, *Lanes 8* and *9*), consistent with the expectation. Thus, a quinuclidin-3-ol moiety was found to be requirement for activation of NADPH oxidase and *GCLC* gene expression. These results, coupled with those presented in Figs. 5–7, were interpreted to indicate that NADPH oxidase activity was required for indole analogue-mediated induction of *GCLC* expression.

DISCUSSION

Mammalian cells contain millimolar concentrations of the tripeptide GSH, which is sequestered in discrete intracellular pools (1, 31, 32). GSH acts as a storage form of cysteine and is a nucleophile as well as an antioxidant. These attributes contribute to the cancer chemoprevention properties of GSH. As an integral component of phase II detoxification metabolism, cytosolic and nuclear GSH participate in the detoxification of genotoxic agents and aid in their efflux (22). GSH is an important component of phase II metabolic detoxification of carcinogenic metals such as arsenite, which can induce VEGF, activate hypoxia-inducible factor 1α, and promote genotoxicity (3, 4). GSH can suppress 12-*O*-tetradecanoylphorbol-13-acetate-stimulated tumor formation and progression (5, 6). Mitochondrial GSH concentrations represent an important mechanism for the detoxification of mitochondrial ROS (33) which can contribute to the high rates of mutation observed in mitochondria (34) found in human neoplasms (35). GSH concentrations can also influence induction of apoptosis, a requirement for maintaining genomic stability by removal of cells containing DNA lesions (36). CD-95 mediated apoptosis has been shown to exhibit a cell-specific requirement for intracellular GSH during caspase-8 activation (37). These reports suggest that GSH can act at various levels to suppress carcinogenesis and represent a rationale for exploring strategies that induce GSH synthesis.

Recently, we found that the indolic drug, indomethacin, enhanced translation of GCL and enhanced GSH synthesis (11). Cells exposed to indomethacin were resistant to diethyl maleate-mediated GSH depletion and cytotoxicity. These indomethacin-mediated effects were a consequence of *GCLC* and *GCLM* mRNA induction, which occurred in a Nrf2-dependent manner (11). Nrf2 is a NF-E2-like basic leucine zipper transcriptional activator and a member of the Cap 'n' Collar basic region leucine zipper family of transcription factors (13). Heterodimeric forms of Nrf2 bind to antioxidant response elements located in the proximal promoters of many phase II genes (38–40). Under basal conditions, Nrf2 is tethered to Keap1 in the cytosol. Recent work performed *in vitro* with purified Keap1 suggests critical cysteine residues in Keap1 located between the BTB domain and the double glycine repeat domains may regulate release of Nrf2 (17). We previously found that exposure to indomethacin caused Keap1 to release Nrf2, allowing free Nrf2 to translocate to the nucleus and induce transcription of *GCLC* and *GLCM* (20). Exposure to antioxidants blocked indomethacin-mediated release of Nrf2 from Keap1, blocked Nrf2 translocation to the nucleus, and blocked transcription of *GCLC* (11). These results suggest that ROS signaling may be essential for Nrf2-mediated induction of *GCLC* by the indole indomethacin.

In this current investigation, we used a series of novel indole analogues and structurally related compounds, and we conducted a comparative structural analysis with the aim of elucidating critical structures responsible for initiating key signaling pathways that contribute to Nrf2 activation of *GCLC*. The analysis indicated that exposure of hepatocellular HepG2 cells to VJ-115, VJ-112-OH, or VJ-175 increased *GCLC* mRNA expression to the same extent as that produced by exposure to indomethacin (Figs. 1 and 9 and Table 1). The structural requirements necessary for the induction of *GCLC* were ascertained. Indomethacin is a 5-methoxy-2-methylindole-3-acetic

acid analogue bearing a *N*-4-chlorobenzoyl substituent, whereas the three active indole analogues (compounds VJ-115, VJ-112-OH, and VJ-175) are 2-indol-3-yl-methylenequinuclidin-3-ols containing either an indolic *N*-benzyl or *N*-benzenesulfonyl substituent. Replacement of the indole ring in these analogues with either a thiophene or a substituted phenyl ring significantly diminished activity by appoximately 85% (VJ-142 and VJ-147; Figs. 1 and 2 and Table 1). This demonstrates that optimal activity was obtained when the indole ring was present in the structure. The presence of an indolic *N*-benzyl or *N*-benzenesulfonyl substituent in these compounds appears to be essential for activity because neither VJ-113 (no indolic *N*-substitution) nor VJ-114 (indolic *N*-methyl substitution) exhibited any activity. The presence of a quinuclidin-3-ol moiety appears to be a requirement for activation of NADPH oxidase and *GCLC* gene expression because replacement of this moiety with a quinulidin-3-one moiety (*i.e.* conversion of the 3-hydroxy group to a 3-keto group) abolished all activity (compare VJ-115 with VJ-111 and VJ-112-OH with VJ-112, Fig. 2). In this present study, competition of the 3-quinuclidin-3-one moiety (VJ-111) with a 3-quinuclidin-3-ol moiety (VJ-115) abrogated induction of *GCLC* mRNA.

An important question is whether the indole compounds screened in this present study act as Michael reaction acceptors in the induction of *GCLC*. Dinkova-Kostova *et al.* (41) have shown that a common chemical feature of many inducers of Nrf2 is a conjugated enone moiety that acts as a Michael reaction acceptor entity. However, none of the active compounds VJ-115, 112-OH, and VJ-175 have this structural entity and therefore can be considered as Michael reaction acceptor compounds. If induction by the indole compounds were solely a function of Michael reaction acceptor activity, then we would expect that VJ-111, VJ-112, and VJ-145, the structures of which all incorporate a conjugated enone system, would induce *GCLC*. However, these compounds did not exhibit any inductive capabilities. Thus, we conclude that induction was not a function of Michael acceptor activity.

Indole analogue-mediated expression of *GCLC* mRNA was shown to be regulated by Nrf2/Keap1 signaling. MEFs derived from Nrf2-null animals were used to show that loss of Nrf2 expression abrogated indole analogue-mediated elevation of *GCLC* message. Keap1 is a negative regulator of Nrf2 (15), sequestering it in the cytosol. Overexpression of Keap1 suppressed indole analogue-mediated enhancement of *GCLC* mRNA.

Indomethacin has been shown to activate the enzyme NADPH oxidase, a source of superoxide production (Refs. 24 and 25; Fig. 4). The activity of NADPH oxidase in HepG2 cell membrane fractions was increased in a linear fashion upon exposure to indole analogues (Fig. 5). This was observed as an increase in membrane translocation of the $p47^{phox}$ subunit (data not shown) and in NADPH oxidase activity. The comparative structure studies indicated that activation of the oxidase required the presence of a hydroxyl group at C3 of the quinuclidine ring of the indole analogues; this same 3-hydroxy substituent is also a structural requirement for *GCLC* induction.

NADPH oxidase is a multisubunit enzyme composed of a membrane flavocytochrome b_{558} complex (a Nox/Duox family member and $gp22^{phox}$) and several cytosolic subunits [Rac, $p67^{phox}$, $p47^{phox}$, and $p40^{phox}$ (25, 26)]. The activated enzyme complex requires translocation of cytosolic subunits to the membrane so that it may catalyze the one-electron reduction of oxygen to superoxide anion using NADPH as a substrate. HepG2 cells express the Nox1 homologue, $p47^{phox}$, and $p67^{phox}$ (27). Expression of NADPH oxidase, specifically Nox2, in phagocytic cells can result in a robust burst of ROS that is used to inactivate bacteria (26). Whereas it is recognized that high levels of ectopic expression of the oxidase in nonphagocytic cells can induce tumorigenicity, low levels of endogenous NADPH oxidase activity are hypothesized to act as an intracellular signal, for example for mitogenic regulation (26). The downstream molecular targets of the oxidase activity are currently unknown but are predicted to contain cysteine residues with a low pK_a (26).

Nrf2-mediated induction of *GCLC* by indomethacin has been shown to be redox regulated (11), in that it could be inhibited by the antioxidant NAC. In untreated HepG2 cells, Nrf2 was found to coimmunoprecipitate with Keap1. Treatment with indomethacin caused Nrf2 to be released from Keap1 and translocate into the nucleus. NAC abolished indomethacin-mediated release of Nrf2 from Keap1 and abolished Nrf2 translocation (11). We have extended those results and now show that the reactivity of Keap1 cysteine sulfhydryls is diminished upon exposure to indomethacin (Figs. 6–8). Indomethacin-mediated loss of thiol reactivity appears to be dependent upon NADPH oxidase activity. Indole-mediated oxidase activation and generation of ROS (11) were found to occur rapidly, preceding thiol oxidation. Conversely, the oxidase inhibitor DPI suppressed indomethacin-mediated changes in Keap1 thiols, when measured by IAA *S*-alkylation. Based on these results, we hypothesize that Keap1 is a downstream effector for NADPH oxidase activity.

Loss of Keap1 thiol reactivity was accompanied by indole analogue-mediated increases in *GCLC* mRNA expression. Inhibition of NADPH oxidase activity by either DPI or PR39 blocked indole analogue-mediated loss of Keap1 thiol reactivity and blocked indole analogue-mediated, Nrf2-dependent elevation of *GCLC* mRNA. These results were interpreted to indicate that exposure of HepG2 cells to the indole analogues activated NADPH oxidase. Increased oxidase activity was accompanied by changes in Keap1 oxidation states, as assessed by reactivity with IAA. Loss of Keap1 thiol reactivity correlated with Nrf2-mediated elevation of *GCLC*. The results obtained *in vivo* are consistent with the work performed *in vitro* and support the hypothesis that Keap1 thiols can act as a molecular sensor of ROS (15, 17).

In summary, we have identified chemical features that maximize indole analogue-mediated activation of Keap1/Nrf2-regulated induction of *GCLC*. Based on these attributes, the functionalized indoles described above may represent potentially novel prototypes for the development of chemopreventive agents for induction of the *GCLC*. In addition, use of the indole analogues has resulted in the identification of NADPH oxidase activity as a novel upstream activity regulating Nrf2/Keap1 signaling, provided data supporting the hypothesis that Keap1 is a downstream effector for oxidase activity, and afforded novel *in vivo* data to support the hypothesis the Keap1 thiols can act as molecular sensors of ROS.

REFERENCES

1. Meister, A. Glutathione metabolism and its selective modification. J. Biol. Chem., *263:* 17205–17208, 1988.
2. McMahon, M., Itoh, K., Yamamoto, M., Chanas, S. A., Henderson, C. J., McLellan, L. I., Wolf, C. R., Cavin, C., and Hayes, J. D. The Cap'n'Collar basic leucine zipper transcription factor Nrf2 (NF-E2 p45-related factor 2) controls both constitutive and inducible expression of intestinal detoxification and glutathione biosynthetic enzymes. Cancer Res., *61:* 3299–3307, 2001.
3. Duyndam, M. C., Hulscher, T. M., Fontijn, D., Pinedo, H. M., and Boven, E. Induction of vascular endothelial growth factor expression and hypoxia-inducible factor 1α protein by the oxidative stressor arsenite. J. Biol. Chem., *276:* 48066–48076, 2001.
4. Maier, A., Schumann, B. L., Chang, X., Talaska, G., and Puga, A. Arsenic co-exposure potentiates benzo[*a*]pyrene genotoxicity. Mutat. Res., *517:* 101–111, 2002.
5. Rotstein, J. B., and Slaga, T. J. Effect of exogenous glutathione on tumor progression in the murine skin multistage carcinogenesis model. Carcinogenesis (Lond.), *9:* 1547–1551, 1988.
6. Perchellet, J. P., Owen, M. D., Posey, T. D., Orten, D. K., and Schneider, B. A. Inhibitory effects of glutathione level-raising agents and D-α-tocopherol on ornithine decarboxylase induction and mouse skin tumor promotion by 12-*O*-tetradecanoylphorbol-13-acetate. Carcinogenesis (Lond.), *6:* 567–573, 1985.

7. De Flora, S., Izzotti, A., D'Agostini, F., and Cesarone, C. F. Antioxidant activity and other mechanisms of thiols involved in chemoprevention of mutation and cancer. Am. J. Med., *91:* 122S–130S, 1991.
8. Martin, K. R., Saulnier, M. J., Kari, F. W., Barrett, J. C., and French, J. E. Timing of supplementation with the antioxidant *N*-acetyl-L-cysteine reduces tumor multiplicity in novel, cancer-prone p53 haploinsufficient Tg.AC (v-Ha-ras) transgenic mice but has no impact on malignant progression. Nutr. Cancer, *43:* 59–66, 2002.
9. Albini, A., Morini, M., D'Agostini, F., Ferrari, N., Campelli, F., Arena, G., Noonan, D. M., Pesce, C., and De Flora, S. Inhibition of angiogenesis-driven Kaposi's sarcoma tumor growth in nude mice by oral *N*-acetylcysteine. Cancer Res., *61:* 8171–8178, 2001.
10. Van Schooten, F. J., Nia, A. B., De Flora, S., D'Agostini, F., Izzotti, A., Camoirano, A., Balm, A. J., Dallinga, J. W., Bast, A., Haenen, G. R., Van't Veer, L., Baas, P., Sakai, H., and Van Zandwijk, N. Effects of oral administration of *N*-acetyl-L-cysteine: a multi-biomarker study in smokers. Cancer Epidemiol. Biomark. Prev., *11:* 167–175, 2002.
11. Sekhar, K. R., Spitz, D. R., Harris, S., Nguyen, T. T., Meredith, M. J., Holt, J. T., Guis, D., Marnett, L. J., Summar, M. L., and Freeman, M. L. Redox-sensitive interaction between KIAA0132 and Nrf2 mediates indomethacin-induced expression of γ-glutamylcysteine synthetase. Free Radic. Biol. Med., *32:* 650–662, 2002.
12. Thun, M. J., Henley, S. J., and Patrono, C. Nonsteroidal anti-inflammatory drugs as anticancer agents: mechanistic, pharmacologic, and clinical issues. J. Natl. Cancer Inst. (Bethesda), *94:* 252–266, 2002.
13. Moi, P., Chan, K., Asunis, I., Cao, A., and Kan, Y. W. Isolation of NF-E2-related factor 2 (Nrf2), a NF-E2-like basic leucine zipper transcriptional activator that binds to the tandem NF-E2/AP1 repeat of the β-globin locus control region. Proc. Natl. Acad. Sci. USA, *91:* 9926–9930, 1994.
14. Wild, A. C., Moinova, H. R., and Mulcahy, R. T. Regulation of γ-glutamylcysteine synthetase subunit gene expression by the transcription factor Nrf2. J. Biol. Chem., *274:* 33627–33636, 1999.
15. Itoh, K., Wakabayashi, N., Katoh, Y., Ishii, T., Igarashi, K., Engel, J. D., and Yamamoto, M. Keap1 represses nuclear activation of antioxidant responsive elements by Nrf2 through binding to the amino-terminal Neh2 domain. Genes Dev., *13:* 76–86, 1999.
16. Zipper, L. M., and Mulcahy, R. T. The Keap1 BTB/POZ dimerization function is required to sequester Nrf2 in cytoplasm. J. Biol. Chem., *277:* 36544–36552, 2002.
17. Dinkova-Kostova, A. T., Holtzclaw, W. D., Cole, R. N., Itoh, K., Wakabayashi, N., Katoh, Y., Yamamoto, M., and Talalay, P. Direct evidence that sulfhydryl groups of Keap1 are the sensors regulating induction of phase 2 enzymes that protect against carcinogens and oxidants. PG-11908–13. Proc. Natl. Acad. Sci. USA, *99:* 11908–11913, 2002.
18. Thomas, J. A., and Beidler, D. A thin-gel isoelectric focusing method for quantitation of protein *S*-thiolation. Anal. Biochem., *157:* 32–38, 1986.
19. Mohazzab, K. M., and Wolin, M. S. Oxidant signalling and vascular oxygen sensing. Role of H_2O_2 in responses of the bovine pulmonary artery to changes in PO_2. Adv. Exp. Med. Biol., *475:* 249–258, 2000.
20. Sekhar, K. R., Yan, X. X., and Freeman, M. L. Nrf2 degradation by the ubiquitin proteasome pathway is inhibited by KIAA0132, the human homolog to INrf2. Oncogene, *21:* 6829–6834, 2002.
21. Courtois, A., Payen, L., Le Ferrec, E., Scheffer, G. L., Trinquart, Y., Guillouzo, A., and Fardel, O. Differential regulation of multidrug resistance-associated protein 2 (MRP2) and cytochromes P450 2B1/2 and 3A1/2 in phenobarbital-treated hepatocytes. Biochem. Pharmacol., *63:* 333–341, 2002.
22. Wolf, C. R. Chemoprevention: increased potential to bear fruit. Proc. Natl. Acad. Sci. USA, *98:* 2941–2943, 2001.
23. Laupeze, B., Amiot, L., Courtois, A., Vernhet, L., Drenou, B., Fauchet, R., and Fardel, O. Use of the anionic dye carboxy-2′,7′-dichlorofluorescein for sensitive flow cytometric detection of multidrug resistance-associated protein activity. Int. J. Oncol., *15:* 571–576, 1999.
24. Tanaka, J., Yuda, Y., and Yamakawa, T. Mechanism of superoxide generation system in indomethacin-induced gastric mucosal injury in rats. Biol. Pharm. Bull., *24:* 155–158, 2001.
25. Bokoch, G. M., and Diebold, B. A. Current molecular models for NADPH oxidase regulation by Rac GTPase. Blood, *100:* 2692–2696, 2002.
26. Lambeth, J. D. Nox/Duox family of nicotinamide adenine dinucleotide (phosphate) oxidases. Curr. Opin. Hematol., *9:* 11–17, 2002.
27. Kikuchi, H., Hikage, M., Miyashita, H., and Fukumoto, M. NADPH oxidase subunit, gp91(phox) homologue, preferentially expressed in human colon epithelial cells. Gene (Amst.), *254:* 237–243, 2000.
28. Li, J. M., and Shah, A. M. Intracellular localization and preassembly of the NADPH oxidase complex in cultured endothelial cells. J. Biol. Chem., *277:* 19952–19960, 2002.
29. Dhakshinamoorthy, S., and Jaiswal, A. K. Functional characterization and role of INrf2 in antioxidant response element-mediated expression and antioxidant induction of NAD(P)H:quinone oxidoreductase 1 gene. Oncogene, *20:* 3906–3917, 2001.
30. Shi, J., Ross, C. R., Leto, T. L., and Blecha, F. PR-39, a proline-rich antibacterial peptide that inhibits phagocyte NADPH oxidase activity by binding to Src homology 3 domains of p47 phox. Proc. Natl. Acad. Sci. USA, *93:* 6014–6018, 1996.
31. Meredith, M. J., and Reed, D. J. Status of the mitochondrial pool of glutathione in the isolated hepatocyte. J. Biol. Chem., *257:* 3747–3753, 1982.
32. Tirmenstein, M. A., and Reed, D. J. Characterization of glutathione-dependent inhibition of lipid peroxidation of isolated rat liver nuclei. Arch. Biochem. Biophys., *261:* 1–11, 1988.
33. Meredith, M. J., and Reed, D. J. Depletion *in vitro* of mitochondrial glutathione in rat hepatocytes and enhancement of lipid peroxidation by adriamycin and 1, 3-bis(2-chloroethyl)-1-nitrosourea (BCNU). Biochem. Pharmacol., *32:* 1383–1388, 1983.
34. Mambo, E., Gao, X., Cohen, Y., Guo, Z., Talalay, P., and Sidransky, D. Electrophile and oxidant damage of mitochondrial DNA leading to rapid evolution of homoplasmic mutations. Proc. Natl. Acad. Sci. USA, *100:* 1838–1843, 2003.
35. Sanchez-Cespedes, M., Parrella, P., Nomoto, S., Cohen, D., Xiao, Y., Esteller, M., Jeronimo, C., Jordan, R. C., Nicol, T., Koch, W. M., Schoenberg, M., Mazzarelli, P., Fazio, V. M., and Sidransky, D. Identification of a mononucleotide repeat as a major target for mitochondrial DNA alterations in human tumors. Cancer Res., *61:* 7015–7019, 2001.
36. Hoeijmakers, J. H. Genome maintenance mechanisms for preventing cancer. Nature (Lond.), *411:* 366–374, 2001.
37. Hentze, H., Schmitz, I., Latta, M., Krueger, A., Krammer, P. H., and Wendel, A. Glutathione dependence of caspase-8 activation at the death-inducing signaling complex. J. Biol. Chem., *277:* 5588–5595, 2002.
38. Chan, J. Y., and Kwong, M. Impaired expression of glutathione synthetic enzyme genes in mice with targeted deletion of the Nrf2 basic-leucine zipper protein. Biochim. Biophys. Acta, *1517:* 19–26, 2000.
39. Kwak, M. K., Itoh, K., Yamamoto, M., Sutter, T. R., and Kensler, T. W. Role of transcription factor Nrf2 in the induction of hepatic phase 2 and antioxidative enzymes *in vivo* by the cancer chemoprotective agent, 3*H*-1,2-dimethiole-3-thione. Mol. Med., *7:* 135–145, 2001.
40. Chanas, S. A., Jiang, Q., McMahon, M., McWalter, G. K., McLellan, L. I., Elcombe, C. R., Henderson, C. J., Wolf, C. R., Moffat, G. J., Itoh, K., Yamamoto, M., and Hayes, J. D. Loss of the Nrf2 transcription factor causes a marked reduction in constitutive and inducible expression of the glutathione *S*-transferase Gsta1, Gsta2, Gstm1, Gstm2, Gstm3 and Gstm4 genes in the livers of male and female mice. Biochem. J., *365:* 405–416, 2002.
41. Dinkova-Kostova, A. T., Massiah, M. A., Bozak, R. E., Hicks, R. J., and Talalay, P. Potency of Michael reaction acceptors as inducers of enzymes that protect against carcinogenesis depends on their reactivity with sulfhydryl. Proc. Natl. Acad. Sci. USA, *98:* 3404–3409, 2001.
42. Tonge, R., Shaw, J., Middleton, B., Rowlinson, R., Rayner, S., Young, J., Pognan, F., Hawkins, E., Currie, I., and Davison, M. Validation and development of fluorescence two-dimensional differential gel electrophoresis proteomics technology. Proteomics, *1:* 377–396, 2001.

NADPH Oxidase Activity Is Essential for Keap1/Nrf2-mediated Induction of *GCLC* in Response to 2-Indol-3-yl-methylenequinuclidin-3-ols

Konjeti R. Sekhar, Peter A. Crooks, Vijayakumar N. Sonar, et al.

Cancer Res 2003;63:5636-5645.